Elektrotechnik & Informationstechnik (2011) 128/3: 75–80. DOI 10.1007/s00502-011-0810-1

ORIGINALARBEIT

Development and test of high-speed bearingless PM synchronous machines

G. Munteanu, A. Binder, T. Schneider

Two high-speed bearingless permanent magnet (PM) synchronous motor prototypes with different mechanical and electrical ratings are presented from the design and performance point of view. For high speed application magnetic bearings are necessary, which in the "bearingless" design are integrated into the active motor part. The first prototype BM-1 was designed for a rotational speed of 60,000 rpm and a mechanical power of 500 W, e.g. as a drive for turbo vacuum pumps. The second prototype BM-2 has an increased mechanical output power of 40 kW at a rated speed of 40,000 rpm, being a suitable drive for compressors and high-speed tooling machines.

Keywords: High-speed electrical machines; PM bearingless motor; magnetic suspension; radial magnetic bearing

Entwicklung und Erprobung von lagerlosen Hochdrehzahl-PM-Synchronmaschinen.

Zwei lagerlose Hochdrehzahl-Permanentmagnet(PM)-Synchronmotorprototypen mit unterschiedlichen mechanischen und elektrischen Bemessungsdaten werden hinsichtlich Auslegung und Betriebsverhalten dargestellt. Bei „lagerlosen" Maschinen ist die für hohe Drehzahlen erforderliche magnetische Lagerung in den Aktivteil der elektrischen Maschine integriert. Der erste Prototyp BM-1 wurde für eine Drehzahl von 60.000 min^{-1} und eine mechanische Leistung von 500 W ausgelegt, z. B. als Antrieb für Turbovakuumpumpen. Der zweite Prototyp BM-2 hat eine erhöhte mechanische Leistung von 40 kW bei einer Bemessungsdrehzahl von 40.000 min^{-1}, was ihn für Kompressoren und Spindelantriebe geeignet macht.

Schlüsselwörter: elektrische Hochdrehzahlmaschinen; PM lagerloser Motor; magnetische Lagerung; Radialmagnetlager

Received October 25, 2010, accepted January 28, 2011

1. Introduction

Gearless drives, called direct drives, for high-speed replace low speed drives with mechanical step-up gears. Therefore, the robustness of the system is increased and the maintenance is reduced. The mechanical power of a rotating machine is proportional to the torque and to the rotational speed. In high speed drives the increase of speed decreases the torque for a given power and therefore, the motor volume decreases, too. Thus, a compacter drive system is achieved. The rotational speed is limited by the bearing system and by the yield strength of the used materials under the action of high centrifugal forces at high speed. The advances in the material science have permitted an increase in the rotational speed by the use of carbon fiber composites (*Binder, Schneider, Klohr, 2005*) as bandage material for synchronous motors with surface mounted permanent rotor magnets. Such a rotor design has proven to be a good choice at high rotational speed (*Binder, Schneider, 2007*).

For rotor bearings special high-speed spindle drive ball bearings e.g. with ceramic balls with minimum oil lubrication can be used, however, they have thermal and mechanical limits. By employing a magnetic suspension much higher speed limits are possible. Usually, the active magnetic suspension is technically implemented as a combination of one axial and two radial magnetic bearings. For the radial bearings vertical and horizontal rotor position must be electronically controlled. Together with the axial direction a five axis controlled rotor suspension is necessary, which is schematically shown in Fig. 1a. Alternatively, with "bearingless" drives the radial magnetic suspension is integrated into the motor active part. So, instead of two radial bearings two parts of bearingless motors are applied.

The bearingless technology can be used with induction machines (*Redemann et al., 2000; Chiba, Power, Rahman, 1995*), switched reluctance machines (*Chen, Hofmann, 2007; Takemoto et al., 2001*) as well as with synchronous machines, especially with PM excitation (*Ooshima et al., 1996; Yajima et al., 2007*). If only one bearingless motor part is used, then a second conventional radial magnetic bearing is necessary (Fig. 1b), except in disc like machines, where a second radial magnetic bearing is not necessary. In all applications with magnetic bearings auxiliary ball bearings with a rotor gap are necessary as a back-up in case of electric faults. In the same way a rotor radial and axial position measurement system is required for the magnetic bearing control.

2. Working principle of bearingless PM drives

The principle of bearingless drives is explained here for PM rotors, but the basic idea applies also to other kinds of bearingless electrical machines, mentioned above. For the torque generation a three phase winding in the stator with the same number of magnetic poles as in the PM rotor is applied, like in conventional AC machines. An example with a two-pole PM motor is schematically given in Fig. 2a. The sum of the radial forces acting between stator and rotor is zero, if no rotor eccentricity occurs. Only tangential forces are acting on the rotor, thus, producing the required torque. A second

Munteanu, Gabriel, Dipl.-Ing., Binder, Andreas, Univ.-Prof. Dr.-Ing. habil. Dr. h.c., Institut für Elektrische Energiewandlung, Technische Universität Darmstadt, Landgraf-Georg-Straße 4, 64283 Darmstadt, Germany; **Schneider, Tobias, Dipl.-Ing.,** Robert Bosch GmbH, Stuttgart, Germany
(E-mail: gmunteanu@ew.tu-darmstadt.de)

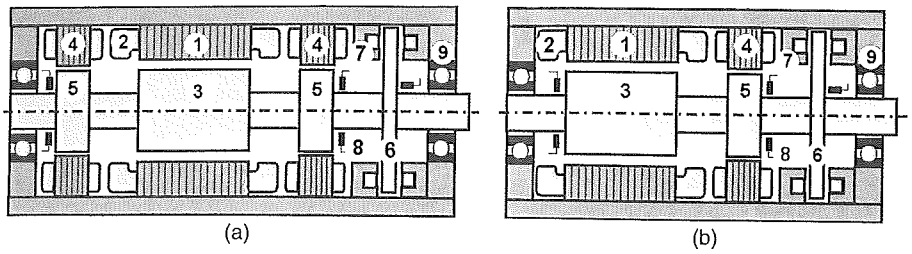

Fig. 1. Schematic drawings of five axis magnetic levitated machines with (a) two radial and one axial magnetic bearing or with (b) one bearingless unit, one radial and one axial magnetic bearing; 1 – motor stator; 2 – winding overhang; 3 – rotor of motor; 4 – radial magnetic bearing stator; 5 – radial magnetic bearing rotor; 6 – axial magnetic bearing disc; 7 – axial magnetic bearing stator; 8 – position sensors; 9 – auxiliary ball bearings

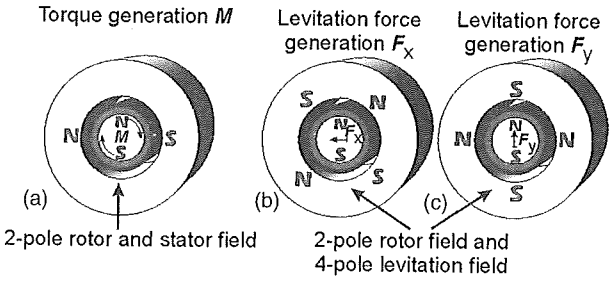

Fig. 2. Principle of a) torque, b) horizontal force and c) vertical force generation with bearingless PM motors

three phase winding is placed in the same stator slots as the motor winding. It generates one magnetic pole pair more or less than the motor winding. In Fig. 2 this levitation winding has four poles, as only one pole pair more is possible with two pole rotors. The sum of the radial forces between the four pole levitation winding and the two-pole PM rotor is no longer zero. It is used for the radial magnetic suspension. In addition tangential magnetic forces between the levitation winding and the rotor magnets occur. Their sum in rotational direction is zero, so they do not produce any torque. But their sum in horizontal and vertical direction is not zero. The direction of these lateral forces depends on the relative position between rotor *d*-axis and levitation field *d*-axis. For example, in Fig. 2b the sum of all magnetic forces acting on the rotor is horizontal, and in Fig. 2c vertical. The motor and the levitation winding in the stator are fed with three phase AC sinusoidal currents with the same electrical frequency. Therefore, the levitation field rotates asynchronously to the rotor field, e.g. with half the speed in Fig. 2. A mathematical description on the force generation in bearingless PM motors is given in (*Schneider, Binder, 2007*).

3. Bearingless motor prototypes

The rotors of both bearingless motor prototypes are suspended by a bearingless unit and a combined axial-radial magnetic bearing (Fig. 1b). The main design parameters of the two prototypes BM-1 and BM-2 are listed in Table 1. In motor BM-1 (Fig. 3) the bearingless unit is situated at the motor drive end (DE), and in motor BM-2 (Fig. 4) at the non-drive end (NDE) for construction reasons. The used rotor radial and axial position sensors are eddy current displacement sensors.

4. Levitation system measurements

Selected measurements are given in the following both for the bearingless levitation system and for the drive system, which are fed from different three phase AC inverters with Pulse Width Modulation. The operation of the combined axial-radial bearing is not discussed.

The radial rotor positions in the horizontal *x*- and vertical *y*-direction have been measured using the feeding inverter control software. The envelopes of the measured *y*-positions in Fig. 5 for BM-1 and in Fig. 7 for BM-2 show at low speed ($n < 6000$ rpm) rather big rotor orbits between 40 and 60 µm, which is roughly one third of the admissible limit. This increased orbit is caused by the common mode rigid body vibration of the rotor in the magnetic bearings. The maximum admissible mechanical air gap in the auxiliary bearings is 150 µm in BM-1 and 180 µm in BM-2.

The no-load tests of the uncoupled machines proved that the rotors of both machines are kept safely within these mechanical constraints, with a 17 µm rotor orbit radius (BM-1, Fig. 6) and a 9 µm rotor orbit radius (BM-2, Fig. 8) at rated rotational speed.

The levitation currents of BM-2 have been measured digitally (8 kHz sampling rate) as *Park*-transformed *d*- and *q*-currents (Fig. 9, rated speed) with the inverter control software. In the *Fourier*

Table 1. Bearingless motor main design parameters

Motor prototype parameter	Symbol	BM-1 Value	BM-2 Value	Unit
Rated mechanical power/rated speed	P_N/n_N	500/60,000	40,000/40,000	W/rpm
Stator inner/outer diameter	d_{si}/d_{sa}	32/60	80/135	mm
Motor winding and PM rotor pole pair count	p_1	1	2	–
Mechanical air gap length	δ_m	1.4	1.5	mm
Magnet height	h_M	3.5	7	mm
Carbon fiber bandage thickness	h_B	1.1	3.5	mm
Levitation winding pole pair count	p_2	2	3	–
Motor/levitation winding rated current	I_1/I_2	9/5	67.13/12	A
Rated levitation force	F_N	10	218	N
Motor/levitation winding rated current loading	A_1/A_2	64/107	192/137	A/cm
Stator cooling method	–	natural cooling	water jacket cooling	–

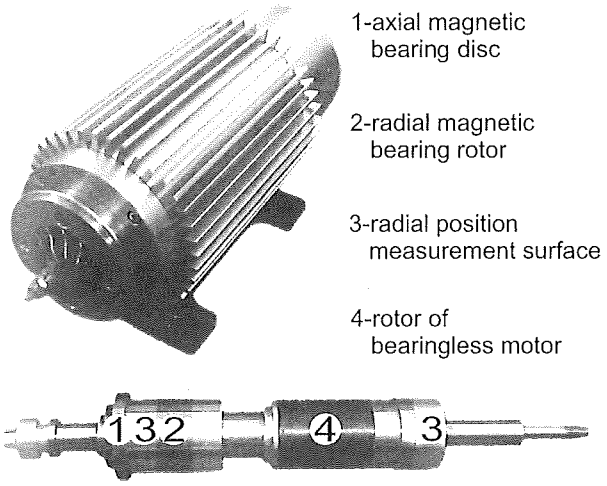

Fig. 3. 500 W bearingless PM motor prototype BM-1, with compressor wheel and its PM rotor

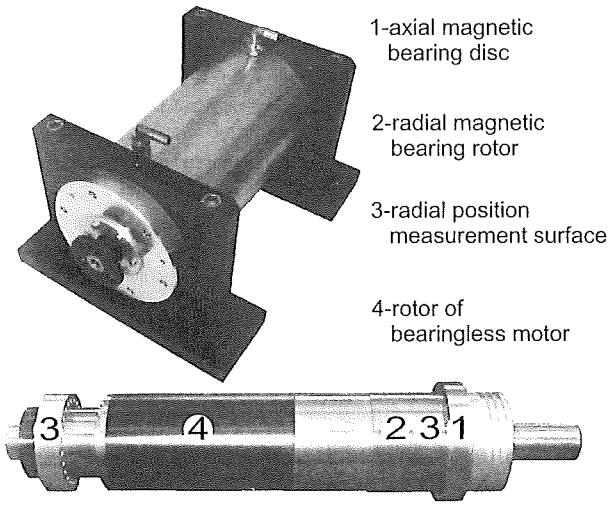

Fig. 4. 40 kW bearingless PM motor prototype BM-2 and its PM rotor

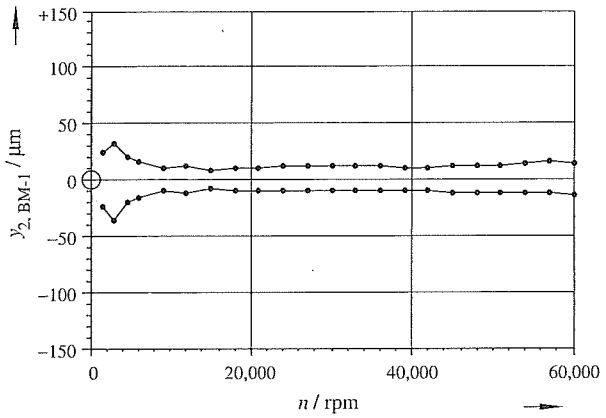

Fig. 5. Measured BM-1 *y*-radial position envelope for the entire speed range

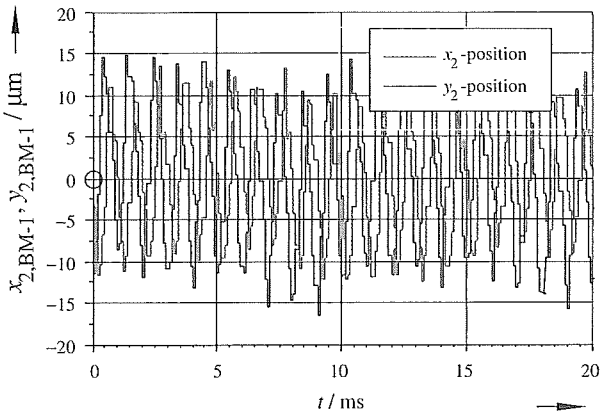

Fig. 6. Measured BM-1 *x*- and *y*-radial positions at motor rated speed $n = 60{,}000$ rpm

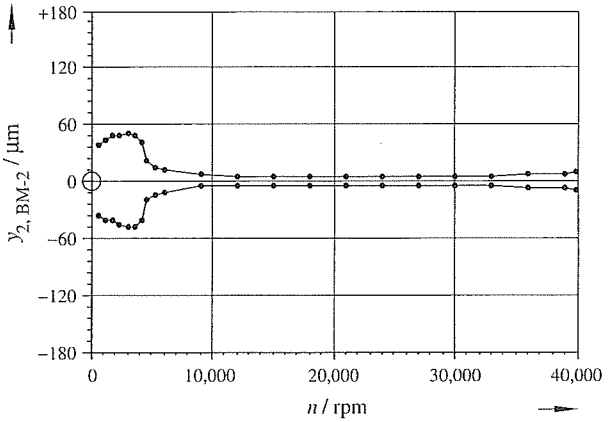

Fig. 7. Measured BM-2 *y*-radial position envelope for the entire speed range

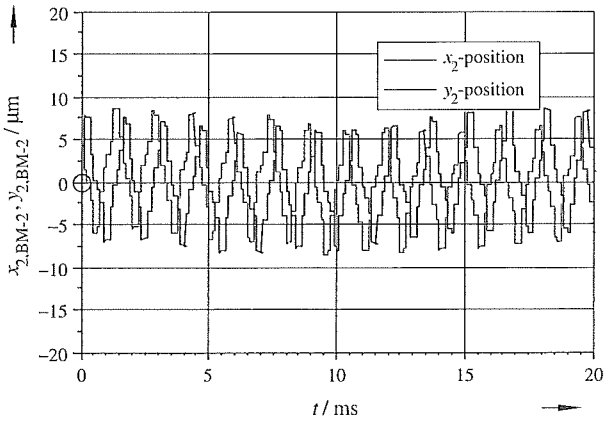

Fig. 8. Measured BM-2 *x*- and *y*-radial positions at motor rated speed $n = 40{,}000$ rpm

spectrum (Fig. 10) of the *d*-current the dominant harmonic is a DC current responsible for the *y*-radial direction magnetic force generation. In the ideal case of constant force generation the *d*-current would be a DC current. However, the measurement shows another harmonic with rotational frequency. This is correlated with the rotor *y*-radial position rotational frequent oscillation around the zero reference position and it is mainly due to the rotor rest mass imbalance.

In order to verify the control of the levitation system the currents have been measured via current transducers directly in the levitation

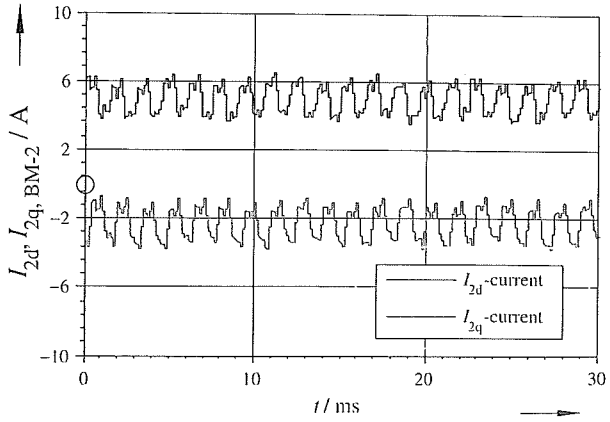

Fig. 9. Measured BM-2 peak *d*- and *q*-levitation currents at rated speed $n = 40{,}000$ rpm

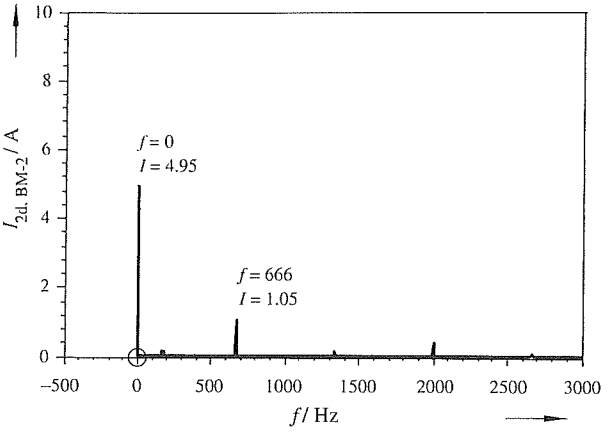

Fig. 10. *Fourier* spectrum of BM-2 peak *d*-levitation current at rated speed $n = 40{,}000$ rpm

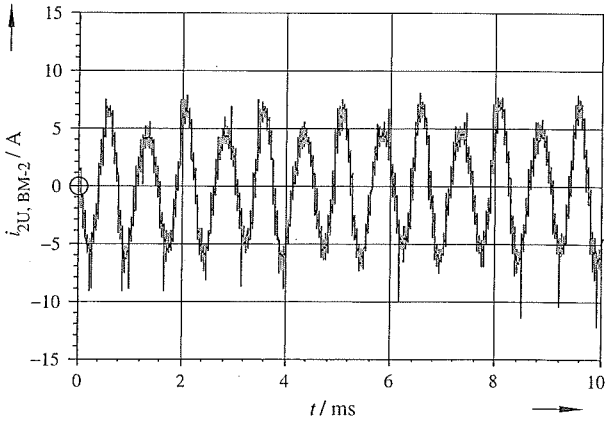

Fig. 11. Measured BM-2 phase *U* levitation current at rated speed $n = 40{,}000$ rpm

winding phase (Fig. 11, rated speed). The levitation current *Fourier* spectrum (Fig. 12) has two main harmonics with: 1332 Hz (motor electrical frequency) and 1998 Hz = 1.5 * 1332 Hz. If the *Park*-transformation is applied to these two current harmonics they become a DC-current and a rotational frequent current, respectively. Thus, the two measurements verify each other.

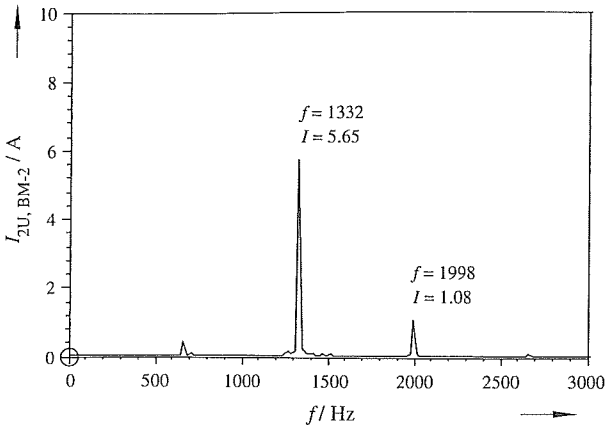

Fig. 12. *Fourier* spectrum of BM-2 phase *U* levitation current at rated speed $n = 40{,}000$ rpm

Motor BM-1 was loaded afterwards with the compressor wheel (Fig. 3) directly mounted on the shaft, showing the same rotor orbit. The motor BM-2 was afterwards elastically coupled with a strain gauge sensor and a second magnetically levitated PM synchronous machine of the same size, with roughly the same rotor orbits. The combined axial-radial magnetic bearing position signals are in the same range.

5. Motor system measurements

In order to verify the motor winding design and the calculated air gap flux density, the back-EMF measurement is performed in the no-load generator mode. For BM-1 a proper driving machine with the same mechanical ratings was not available. Therefore, the measurement of the back-EMF as no-load generator stator voltage was performed up to 13,660 rpm, using compressed air and the rotor compressor wheel as a driving unit. As the back-EMF rises linear with speed, it was linear extrapolated to 60,000 rpm (Fig. 13). Motor BM-2 was driven by the coupled load machine up to 36,000 rpm and linear extrapolated to 40,000 rpm (Fig. 14). The phase back-EMF r.m.s. results at rated speed are: BM-1: 18.8 V/18.5 V, measured/calculated, BM-2: 223.5 V/220.3 V. In order to determine the motor no-load losses by deceleration test, at rated speed the motor winding supply inverter is turned off, and the rotor decelerates freely to zero speed. The rotor kinetic energy is transformed into air friction losses, stator iron core losses due to the rotor PM field, rotor eddy current losses due to the magnetic field of the levitation winding and

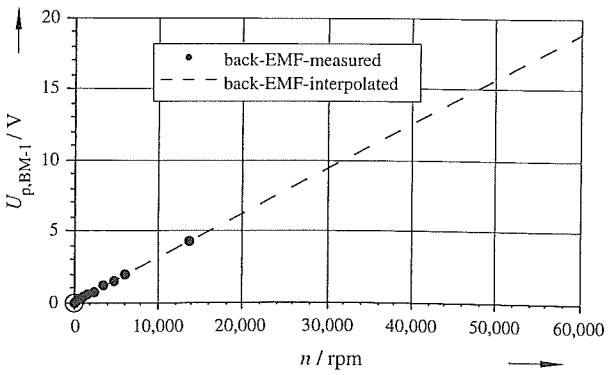

Fig. 13. Measured back-EMF of BM-1 up to 13,360 rpm and extrapolated to 60,000 rpm

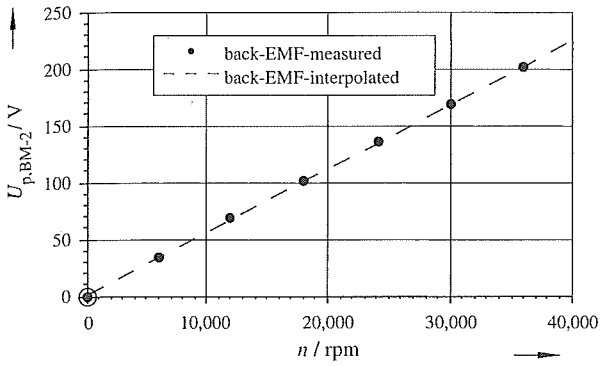

Fig. 14. Measured back-EMF of BM-2 up to 36,000 rpm and extrapolated to 40,000 rpm

rotor losses in the axial-radial magnetic bearing. The accurate value of the rotor inertia is important for the measurement evaluation.

In a next step, the sum of the no-load losses was measured via electrical input power. Afterwards, both prototypes have been tested under mechanical load and different speed. Due to the driving stator field the resistive I^2R (I being the motor phase current and R the winding phase DC resistance) losses, the eddy current losses in the motor winding, the stator iron core, rotor core and magnet losses increase with load. The switching frequency of the two-level voltage source inverters for BM-1 is 20 kHz/40 kHz for the motor/levitation winding. For BM-2 a three-level motor inverter with 64 kHz was used, and a two level inverter with 16 kHz switching frequency for the levitation winding, so for both motors no output filter was necessary. Only the input electrical power of BM-1 which was operated as a compressor drive was measured (Fig. 15). Via the torque sensor the output mechanical power of BM-2 was measured together with the input electrical power until now up to 30,000 rpm for BM-2 (Fig. 16). All these measurements are done at thermal steady-state conditions to check the cooling system. For example, at rated torque and 30,000 rpm the steady state temperature was 108 °C in the rotor magnets, 80 °C in the stator windings at 35.2 °C water inlet temperature and 8 l/min water flow rate.

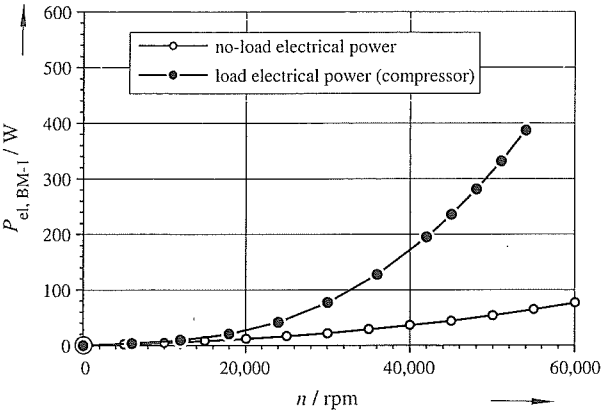

Fig. 15. Measured BM-1 no-load input electrical power and load (compressor wheel) input electrical power

A precise calculation of the losses in high speed drives is difficult due to the air friction losses and the additional winding losses due to current displacement in randomly distributed round wire coils. These types of losses were determined analytically for both prototypes. The calculated total losses of BM-1 (*Schneider, Binder, 2010*) are 86 W at rated power, yielding a motor efficiency of 85.3% not including the

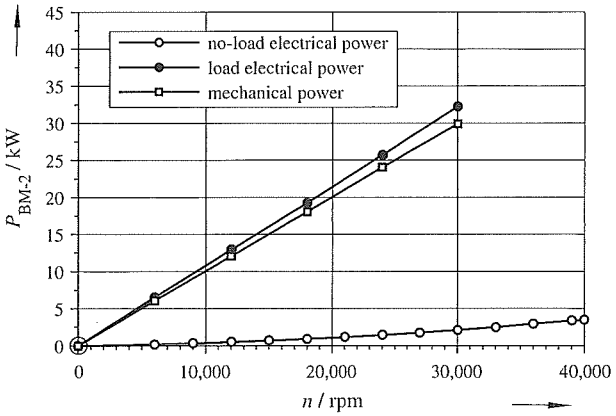

Fig. 16. Measured BM-2 no-load input electrical power, load input electrical power and output mechanical power

inverter and the axial-radial magnetic bearing. The measured total losses of BM-2 are 2162 W at 30,000 rpm and 9.51 Nm, yielding a motor efficiency of 93.3%. The calculated losses are with 1963 W ca. 10% lower.

6. Conclusions

The bearingless motors share the same advantages as motors with conventional magnetic bearings, but have some additional benefits. Together with a combined axial-radial magnetic bearing a slightly shorter motor shaft is possible, thus, the motor reaches a higher speed without passing through the first critical speed due to the first bending mode. Standard iron laminations and standard AC power converters are used with bearingless drives in comparison to conventional magnetic bearings, which need special stator and rotor iron laminations and DC power electronics. Although the rotor losses of the bearingless PM motor are due to the asynchronously rotating levitation field, these losses are usually lower than in the hetero-polar radial magnetic bearings. So the rotor temperature is kept lower in bearingless machines. This is a considerable advantage as an increased rotor temperature decreases the rotor magnet demagnetization limit and may endanger the safe mechanical operation of the carbon fiber bandage. The performances of both presented high-speed bearingless motor prototypes show that they are a good alternative to the conventional magnetic suspension. Up to now this kind of high speed motor has been experimentally investigated only in the low power range below 100 kW, so future work will focus on higher power ratings.

References

Binder, A., Schneider, T. (2007): High-speed inverter-fed AC drives. Int. Aegean Conf. on Electrical Machines and Power Electronics, ACEMP '07, pp. 9–16.

Binder, A., Schneider, T., Klohr, M. (2005): Fixation of buried and surface-mounted magnets in high-speed permanent-magnet synchronous machines. IEEE Transactions on Industry Applications, 42 (4): 1031–1037.

Chen, L., Hofmann, W. (2007): Performance Characteristics of one Novel Switched Reluctance Bearingless Motor Drive. PCC'07 Power Conversion Conf., Nagoya, Japan, pp. 608–613.

Chiba, A., Power, D. T., Rahman, M. A. (1995): Analysis of no-load characteristics of a bearingless induction motor. IEEE Transactions on Industry Applications, (1): 77–83.

Ooshima, M., et al. (1996): Design and analysis of permanent magnet-type bearingless motors. IEEE Transactions on Industrial Electronics, 43 (2): 292–299.

Redemann, Ch., et al. (2000): 30 kW Bearingless Canned Motor Pump on the Test Bed. 7th Int. Symp. on Magnetic Bearings, Zürich, Switzerland, pp. 189–194.

Schneider, T., Binder, A. (2007): Design and evaluation of a 60,000 rpm permanent magnet bearingless high speed motor. 7th Int. Conference on Power Electronics and Drive Systems PEDS '07, pp. 1–8.

Schneider, T., Binder, A. (2010): Entwicklung und experimentelle Untersuchung eines lagerlosen permanenterregten Synchron-Hochdrehzahlmotors für 60,000/min. 8. ETG/GMM-Fachtagung „Innovative Klein- und Mikroantriebstechnik", 22.–23. Sept. 2010, Würzburg, Germany, pp. 31–36.

Takemoto, M., et al. (2001): Improved analysis of a bearingless switched reluctance motor. IEEE Transactions on Industry Applications, 37 (1): 26–34.

Yajima, S., et al. (2007): Total Efficiency of a Deeply Buried Permanent Magnet Type Bearingless Motor Equipped with 2-pole Motor Windings and 4-pole Suspension Windings. IEEE Power Engineering Society General Meeting, Tampa, FL, USA, pp. 1–7.

Authors

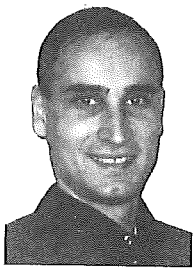

Gabriel Munteanu
received his Dipl.-Ing degree from "Politehnica" University of Bucharest, Romania, in September 2006. Since August 2007 he has been a Ph.D. student at the Institute for Electrical Energy Conversion at Darmstadt University of Technology, Germany. His current research is focused on magnetically levitated electric drives.

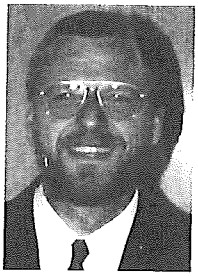

Andreas Binder
received the Dipl.-Ing. (diploma) and Dr. techn. (Ph.D.) degree in Electrical Engineering from the Vienna University of Technology, Vienna, Austria, in 1981 and 1988, respectively. From 1981 to 1983 he was with the ELIN-Union AG, Vienna, working on synchronous generators design. From 1983 to 1989 he joined the Department of Electrical Machines and Drives, Vienna University of Technology, as researcher. From 1989 to 1997 he led a group, developing DC and inverter-fed AC motors and drives, at Siemens AG, Bad Neustadt and Erlangen, Germany. Since 1994 he has been lecturer at the Vienna University of Technology, Vienna, Austria (venia docendi). In 1997 he received the ETG-Literature Award of German Assoc. of Electrical Engineers VDE. Since October 1997 he has been Head of the Institute of Electrical Energy Conversion, Darmstadt University of Technology, as a full professor, being responsible for teaching and research for electrical machines, drives and railway systems. He is the author or co-author of more than 240 scientific publications and holds several patents. Andreas Binder is Senior Member of IEEE and Member of VDE, IEE, VDI and EPE.

Tobias Schneider
received his Dipl.-Ing. degree from Darmstadt University of Technology, Darmstadt, Germany in September 2002. From 2002 to 2008 he was a Ph.D. student at the Department of Electrical Energy Conversion at Darmstadt University of Technology, where he was involved in research on bearingless motors in high speed applications. He is now working for Robert Bosch GmbH, Stuttgart, Germany. Tobias Schneider is member of VDE.